Summary of G1 group in 2013

H. Yamanaka

RECENT ACTIVITIES

1. Estimation of effects of slope topography in Lima
2. Strong motion simulation in Lima for future large earthquakes
3. Empirical estimation of site amplifications in Lima
4. S-wave velocity exploration of deep soil in Tacna

Effects of Irregular Topography on the Dynamic Response of a Populated Slope in Lima City

2. Estimation of Dynamic Properties along the Slope (1/5).

A **target populated slope** was chosen in the district of Independencia.

Seven microtremor array measurements were conducted along the slope line A-A'. Due to **space limitations**, locations of the tests were restricted to open spaces like parks in the flat level and **only small circles or linear arrays for tests in the slope**.

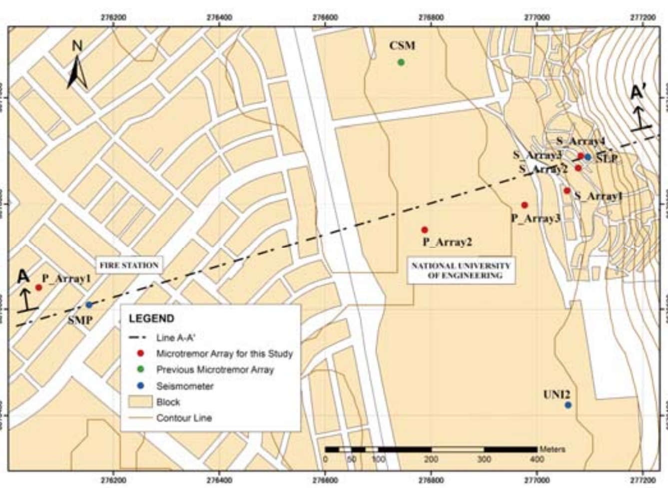

2. Estimation of Dynamic Properties along the Slope (2/5).

Dispersion curves of surface waves were calculated for each of the sites. Since a **continuous trend between the linear and circular arrays** was found, and due to the space limitations, **only linear arrays** were conducted for **S_Array4**.

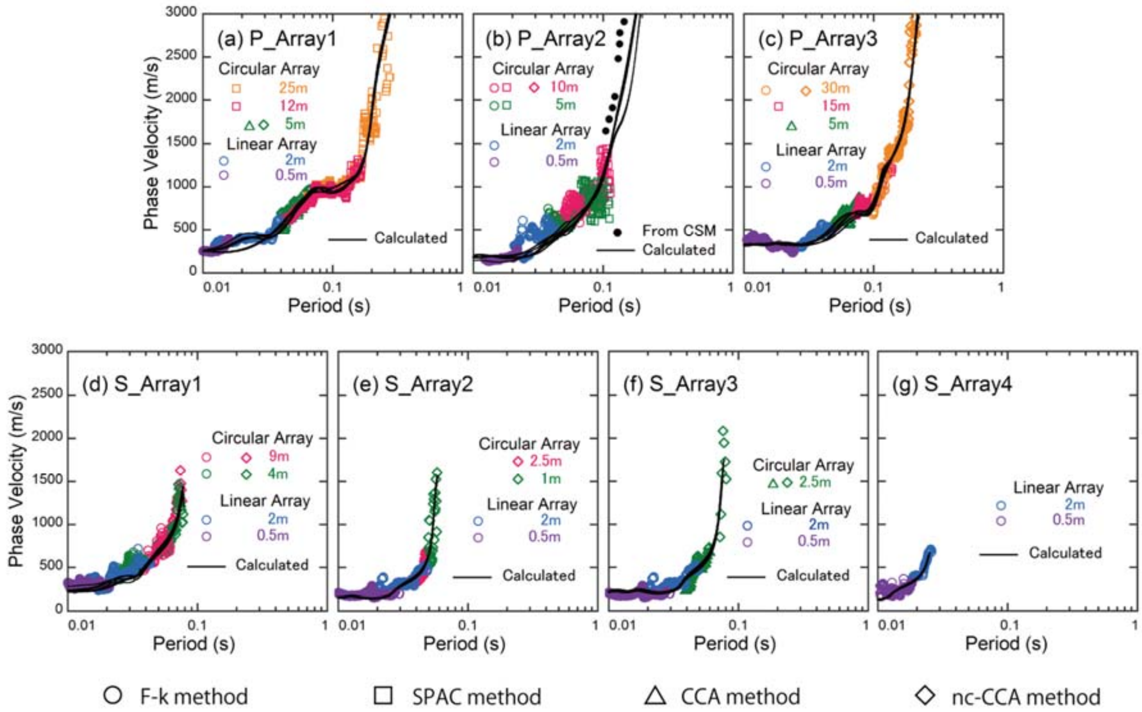

2. Estimation of Dynamic Properties along the Slope (3/5).

The **Genetic Algorithms (GA)** were adopted as **nonlinear optimization method** in this case. Due to the non-uniqueness of the solution, the inversion analysis was performed **five times** for each of the sites.

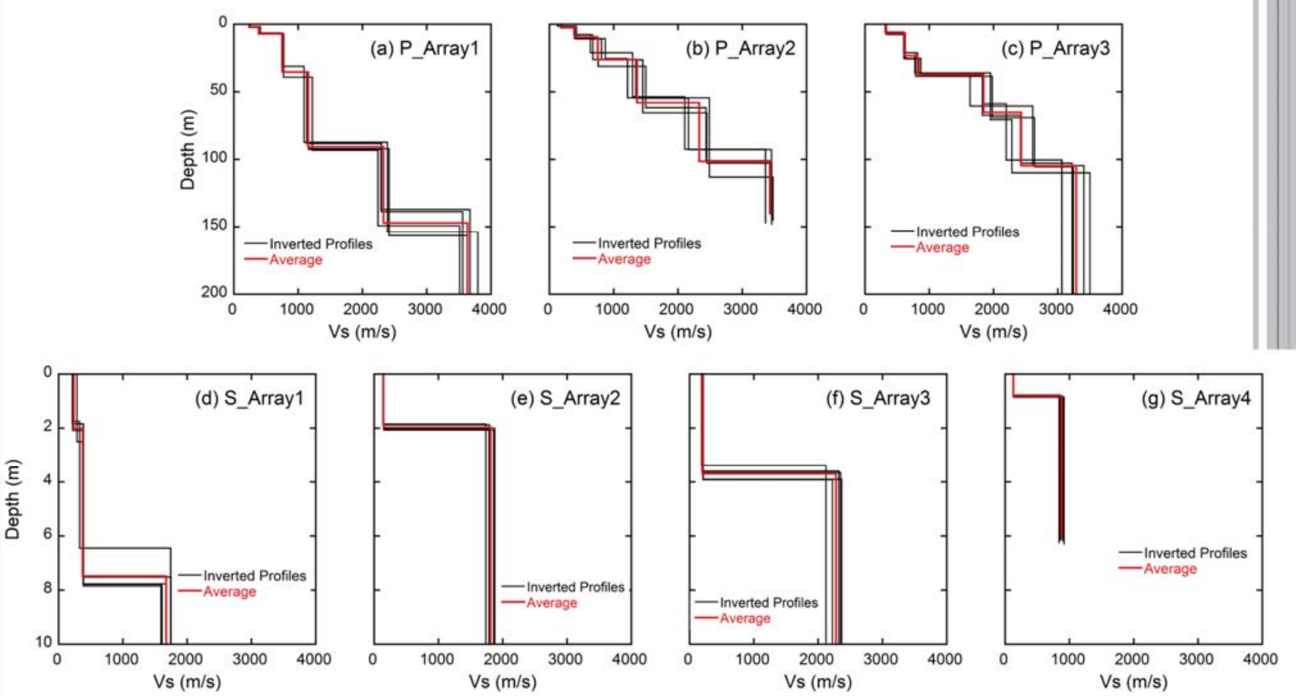

2. Estimation of Dynamic Properties along the Slope (4/5).

Results showed a **reduction of the depth to the bedrock** while approaching the foothill and the presence of a **shallow layer with poor dynamic properties** in the sloping areas. It is a fact that **this problem also occurs at other populated slopes**.

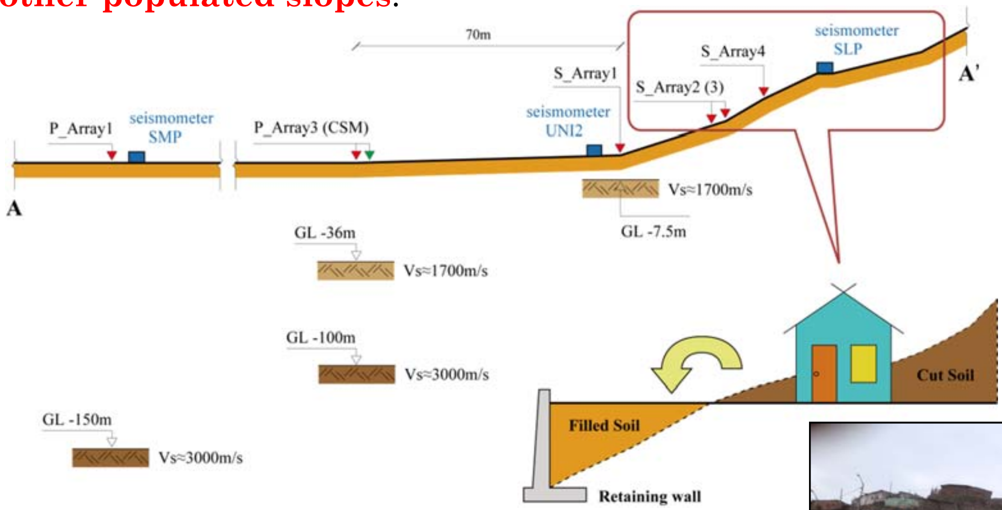

2. Estimation of Dynamic Properties along the Slope (5/5).

An seismometer was installed in the slope (**SLP**) to compare the seismic records with the ones installed in the flat area (**SMP and UNI2**)

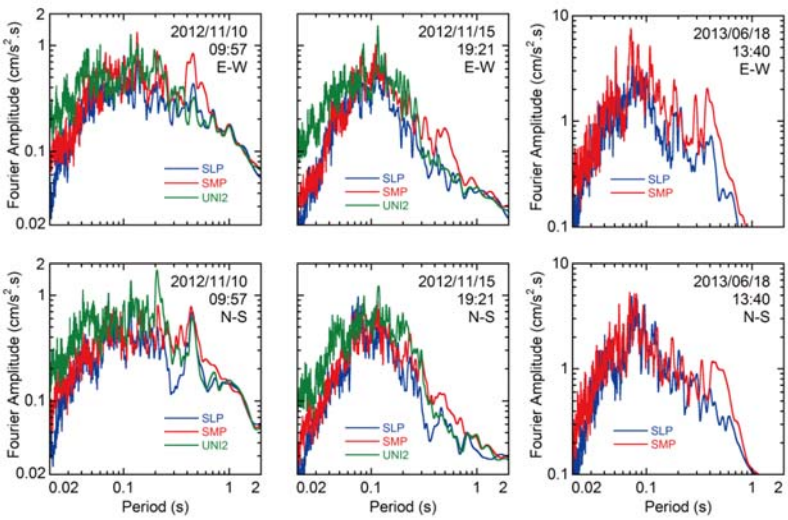

Date	Local time	Longitude (deg.)	Latitude (deg.)	Magnitude (ML)	Depth (km)	Hypocentral distance to SMP (km)	Peak Ground Acceleration (cm/s^2)		
							SMP	UNI2	SLP
2012/11/10	09:57	-8.89	-75.12	6.0	146	431	2.60	4.07	2.29
2012/11/15	19:21	-13.30	-76.68	4.8	57	158	2.72	2.93	1.94
2013/06/18	20:57	-12.04	-77.66	5.1	40	40	33.97	---	26.10

3. Finite Element Model (3/6).

Quadrilateral shapes were used but in specific cases, such as in the transition to outcropping materials, **triangular elements** were generated.
The problem was solved for **plane strain** conditions.

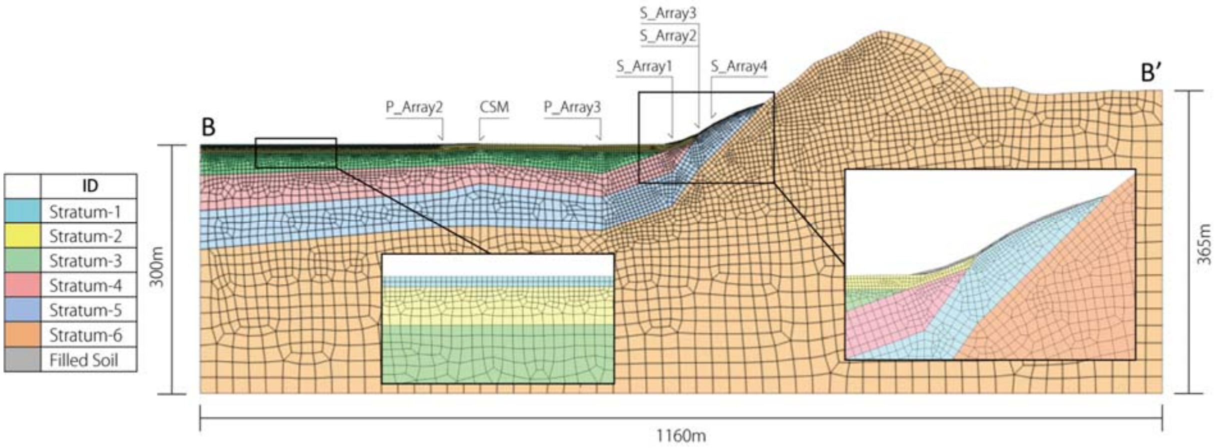

	ρ (kg/m³)	V_S (m/s)	G (MPa)	υ	V_P (m/s)	Damping ratio
Stratum-1	1700	212	77	0.25	368	0.030
Stratum-2	1800	384	265	0.25	664	0.020
Stratum-3	1800	733	967	0.20	1197	0.010
Stratum-4	2200	1623	5794	0.14	2508	0.004
Stratum-5	2200	2405	12720	0.14	3716	0.003
Stratum-6	2600	3504	31916	0.17	5556	0.002
Filled Soil	1500	176	47	0.35	367	0.040

3. Finite Element Model (2/6).

Synthetic accelerograms were calculated up to the surficial soil for **8 sites** where 1-D shear-wave velocity profiles are available (Pulido, 2013).
The simulated waveform for CSM for the **most critical slip** was **deconvulated** in order to obtain the **input motion at the bottom layer**.

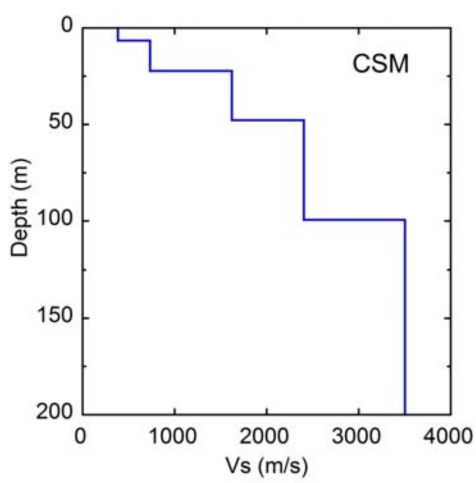

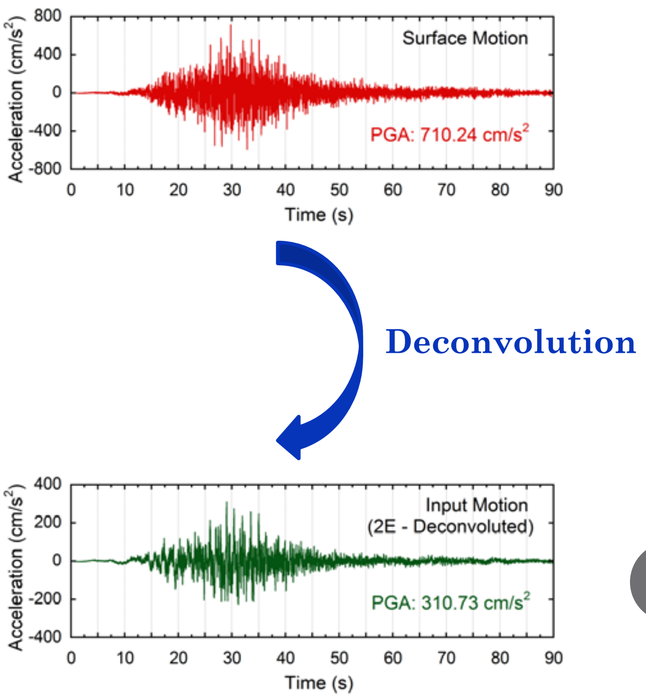

3. Finite Element Model (5/6).

From the distribution of the **absolute values of PGA** of the **horizontal motion** for the entire model it can be observed that **amplification of the response is evident for surface layers in the flat areas** and no larger values can be found on the sloping areas of the model.

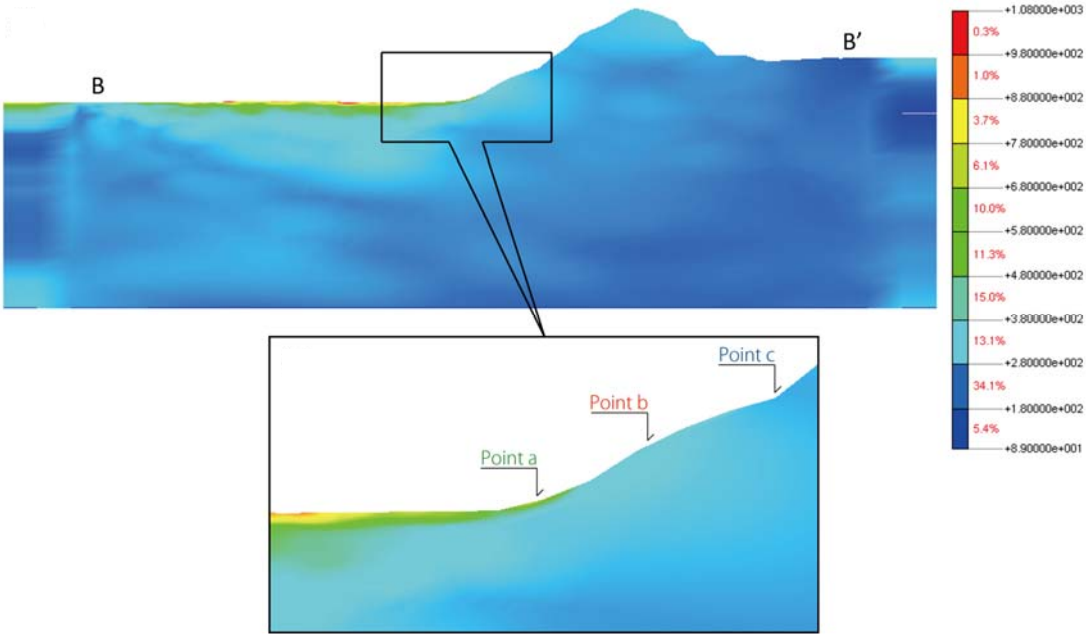

3. Finite Element Model (6/6).

Results showed that **larger PGA** (~600cm/s²) is obtained for areas close to the **foot of the slope** (Point a) as well as a **sharp peak in the vicinity of 0.06s** in the velocity response spectrum.

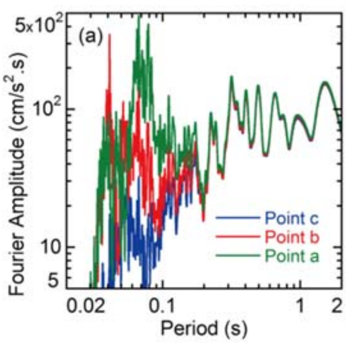

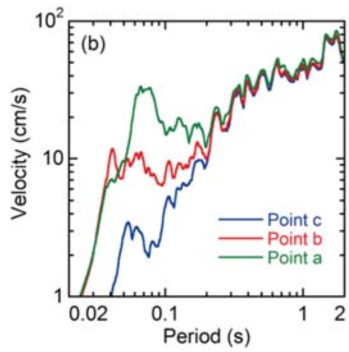

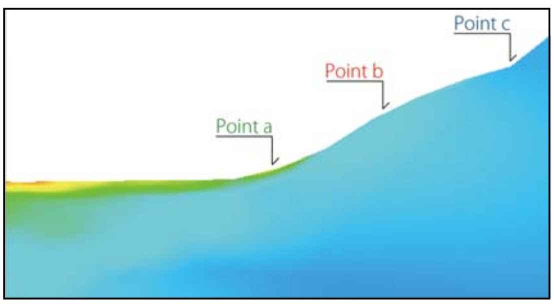

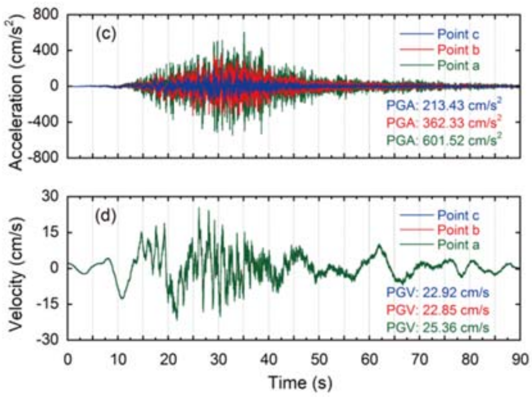

Earthquake rupture and slip scenarios for Central Andes Peru, and strong motion simulations for Lima

Slip deficit rate for Peru and Northern Chile and scenario earthquake for Central Peru

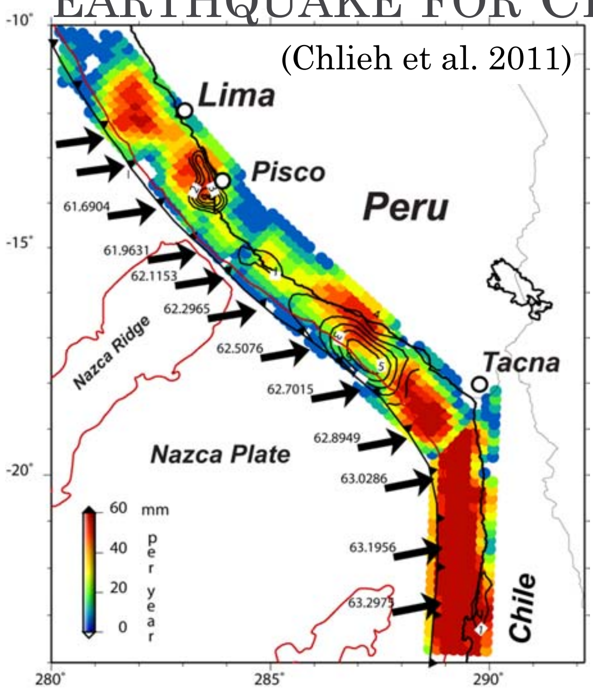

$C(x)_* vo$

- Slip deficit since 1746 (265 years)
- Maximum slip is 20 m
- Magnitude Mw~8.9, neglecting the 20 century earthquake

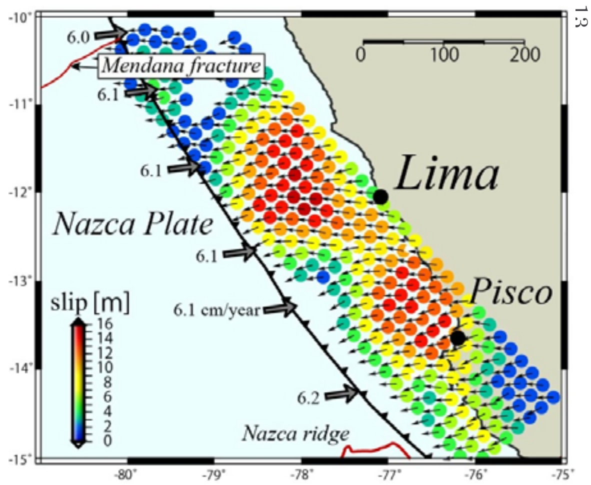

$S(x)=C(x)_* vo_* t$

(Pulido et al. 2011)

S(x): slip, t : elapsed time

EARTHQUAKE SLIPS SCENARIOS FOR CENTRAL PERU

obtained from geodetic data, as well as information of recurrence of historical earthquakes (Pulido 2013)

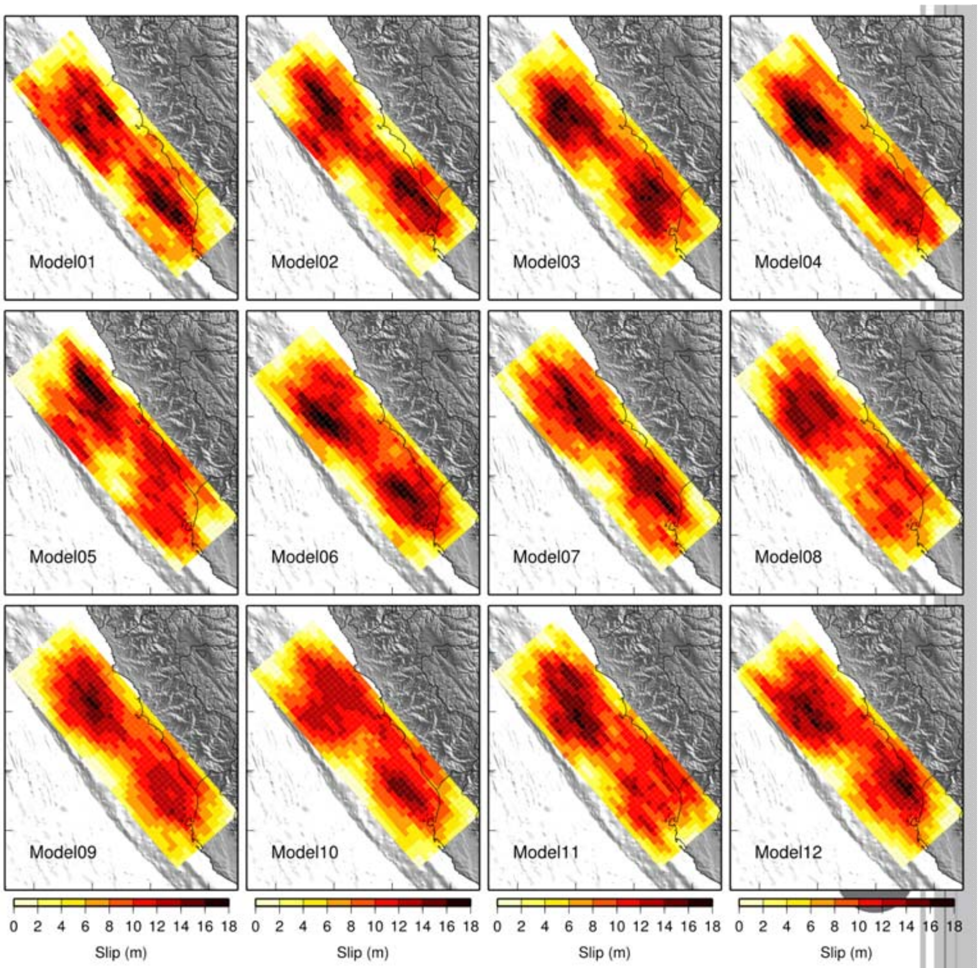

http://www.j-

HYPOCENTER LOCATIONS SCENARIOS

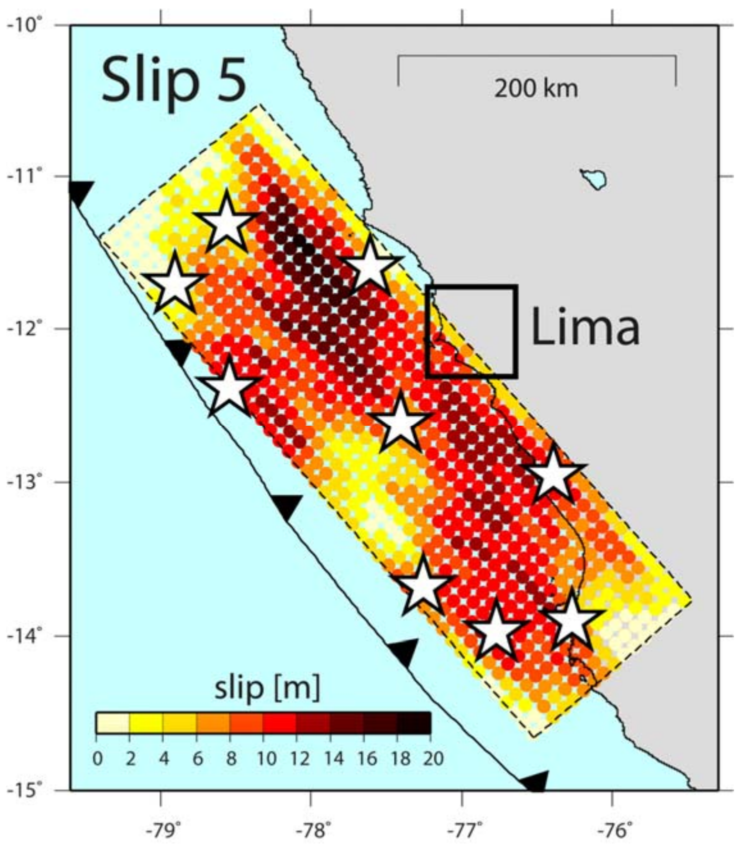

AVERAGE S-WAVE VELOCITY FOR THE UPPER 10M AND SOIL AMPLIFICATIONS TO ENGINEERING BEDROCK (VS ~ 400M)

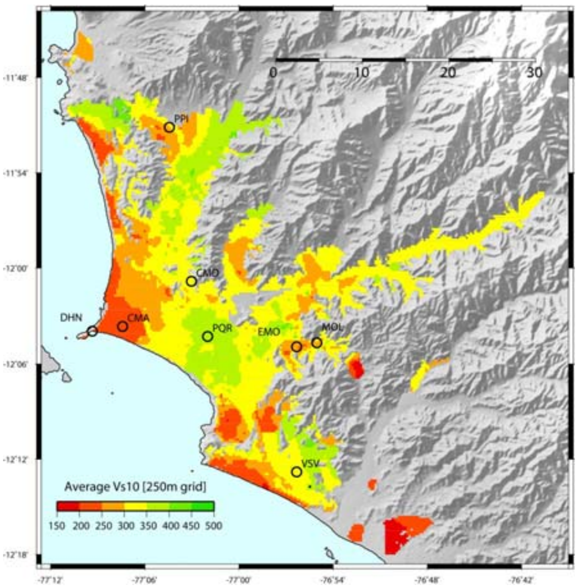

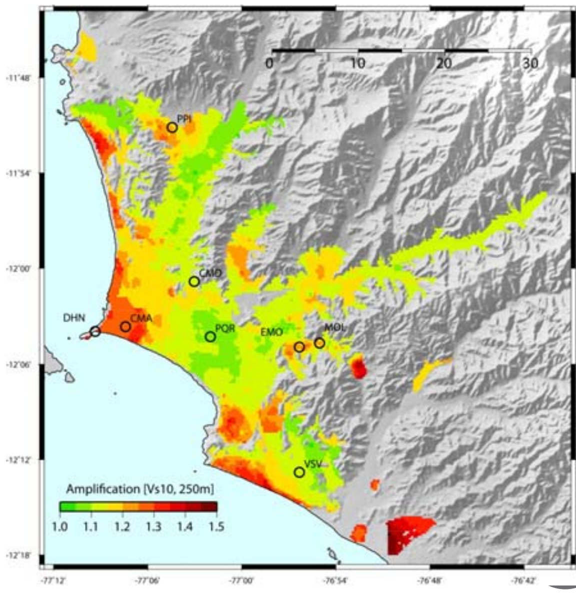

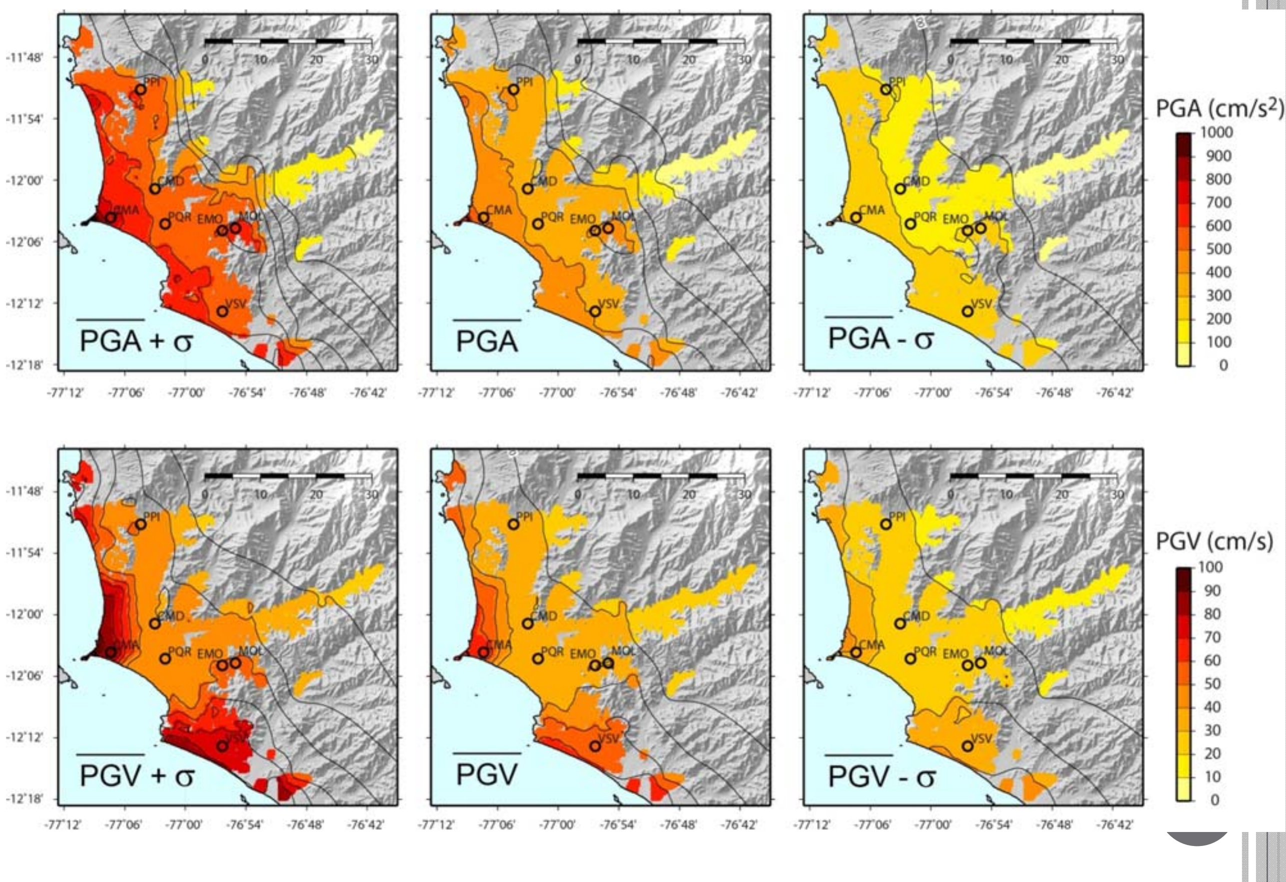

AVERAGE PSEUDO ACCELERATION RESPONSE SPECTRA (PSA) FOR ALL SCENARIOS AND SELECTED PERIODS (H=0.05)

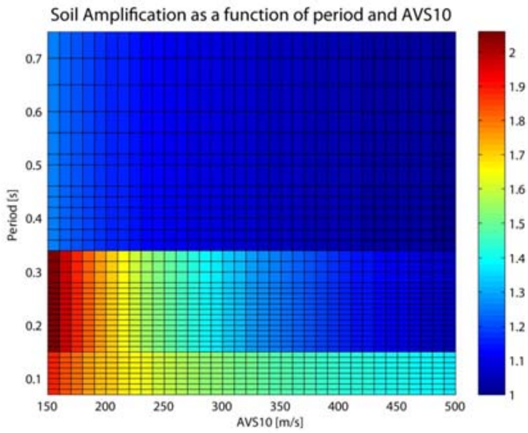

Frequency dependent site amplifications (Sekiguchi et al. 2013)

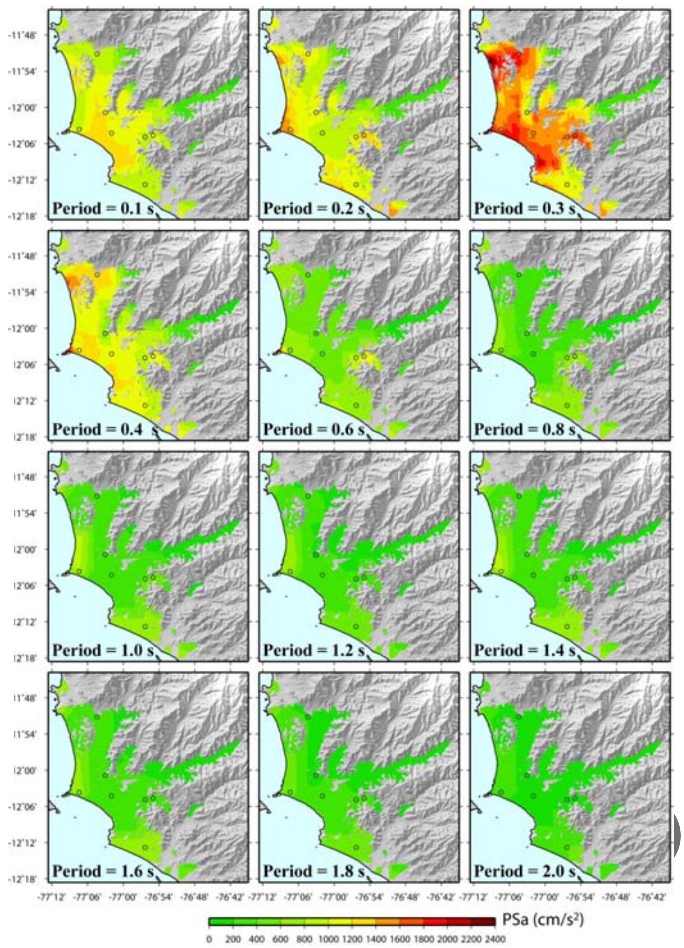

Analysis strong motion records in city of Lima

1- DATA

222 records at CISMID and IGP strong motion sites were used in spectral separation to source, path and site effects

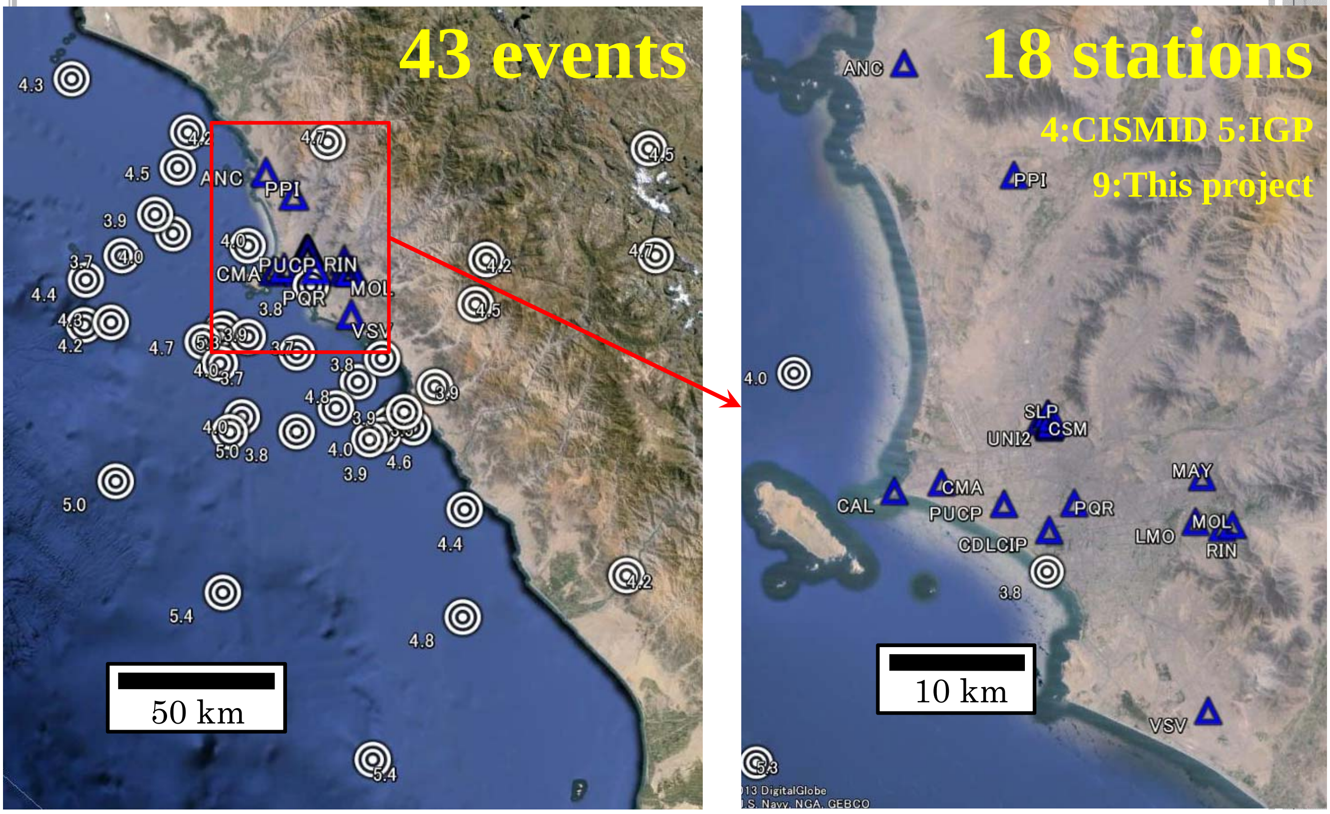

2- RESULTS:

Qs-value of propagation path in crust and mantle

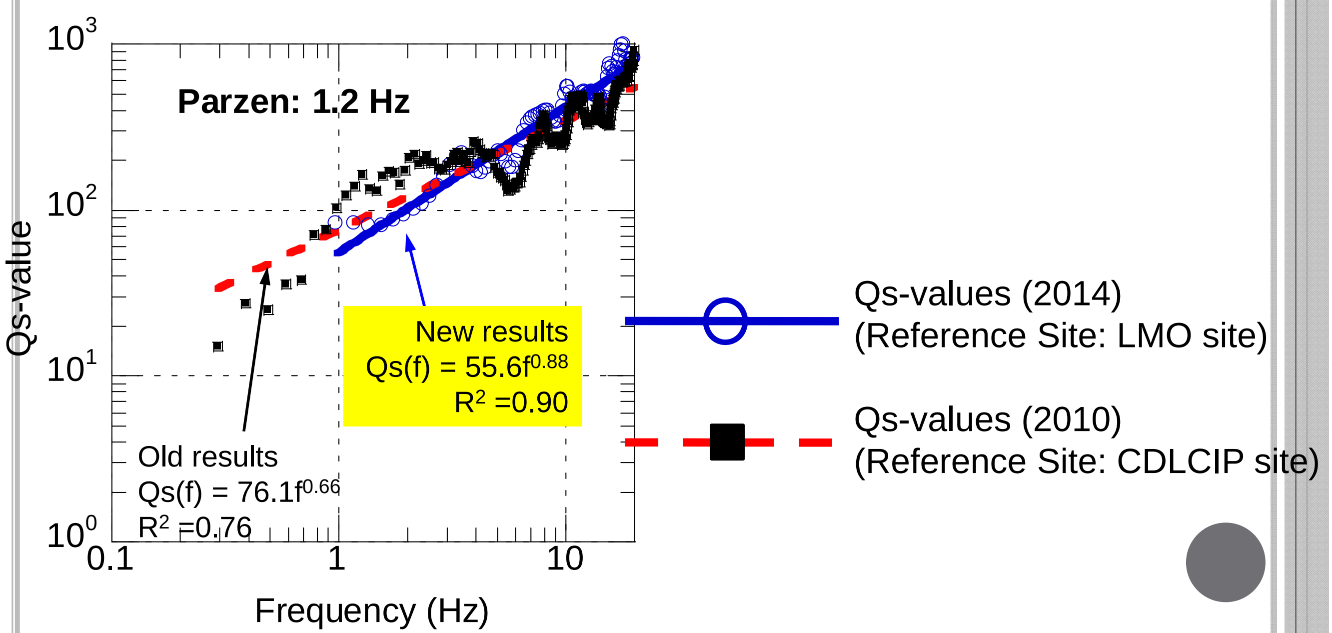

2- RESULTS: Site amplifications at 18 sites

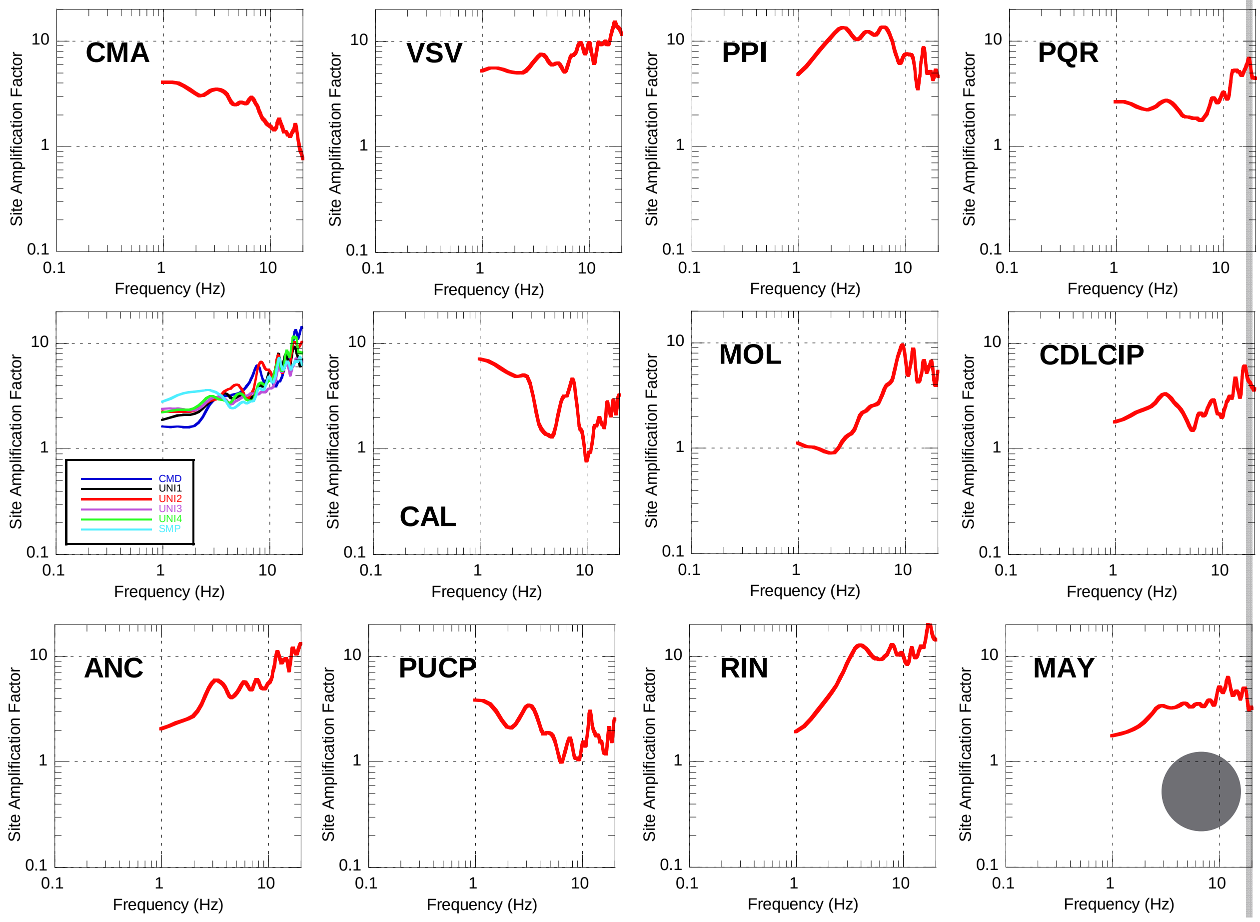

2- RESULTS: Comparison – CMA site

Standard spectral ratio (SSR)

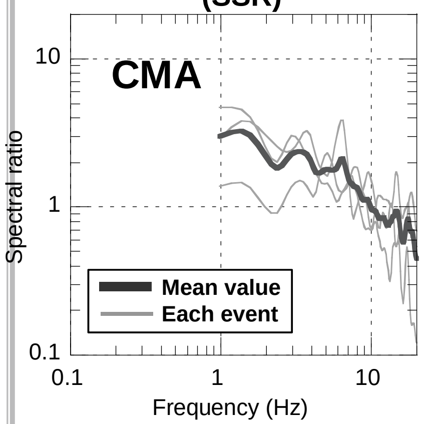

Horizontal to vertical spectral ratio (HVSR)

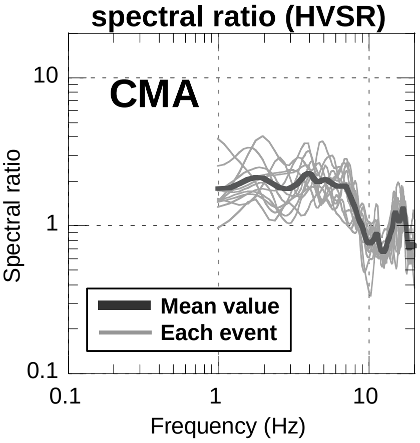

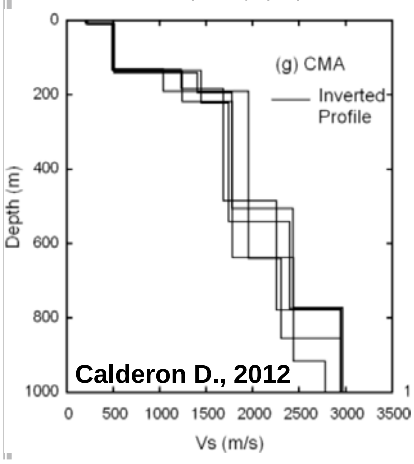

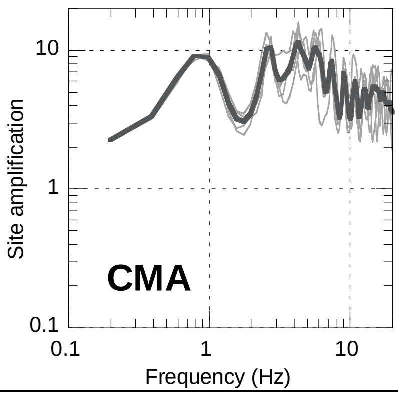

Mean value
1-D theoretical computation for each profile

Spectral inversion method
SSR method
HVSR method
1-D theoretical computation

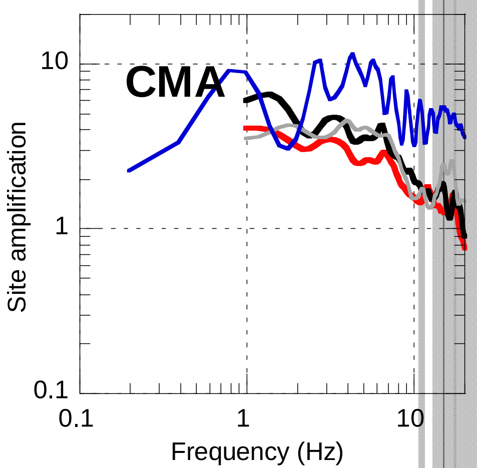

Estimation of Q-values of soil from amplification

CMA

$$Q = \begin{cases} \frac{Vs}{120} f^{0.66} & f \leq 17.4Hz \\ \frac{Vs}{120} 17.4^{0.66} & f > 17.4Hz \end{cases}$$

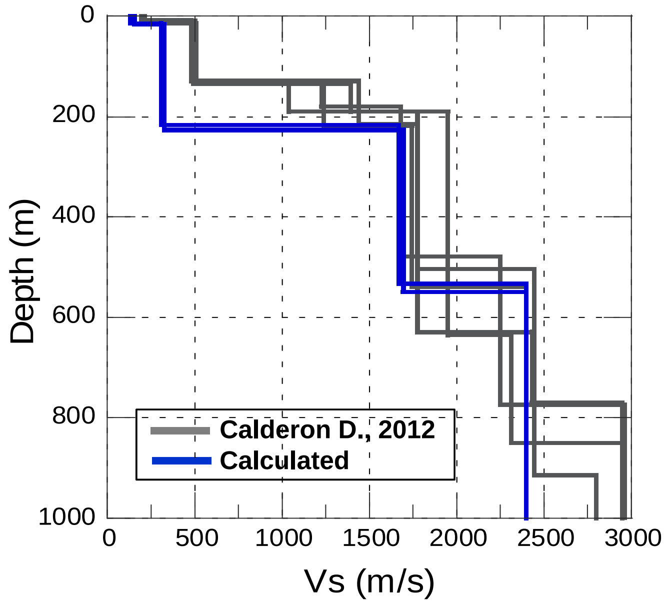

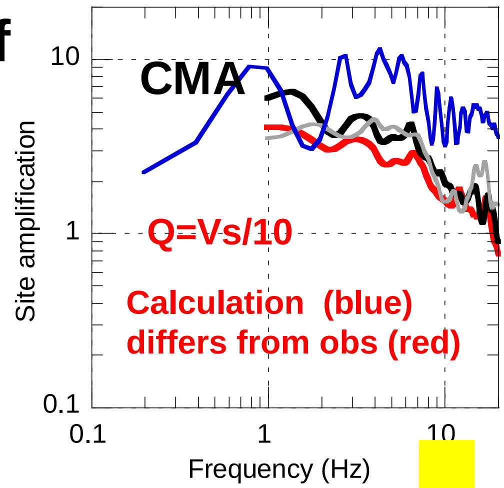

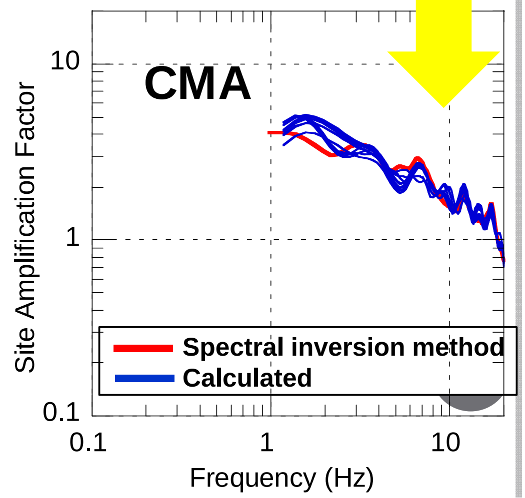

S-wave velocity profiles at the city of Tacna

1. Location map.

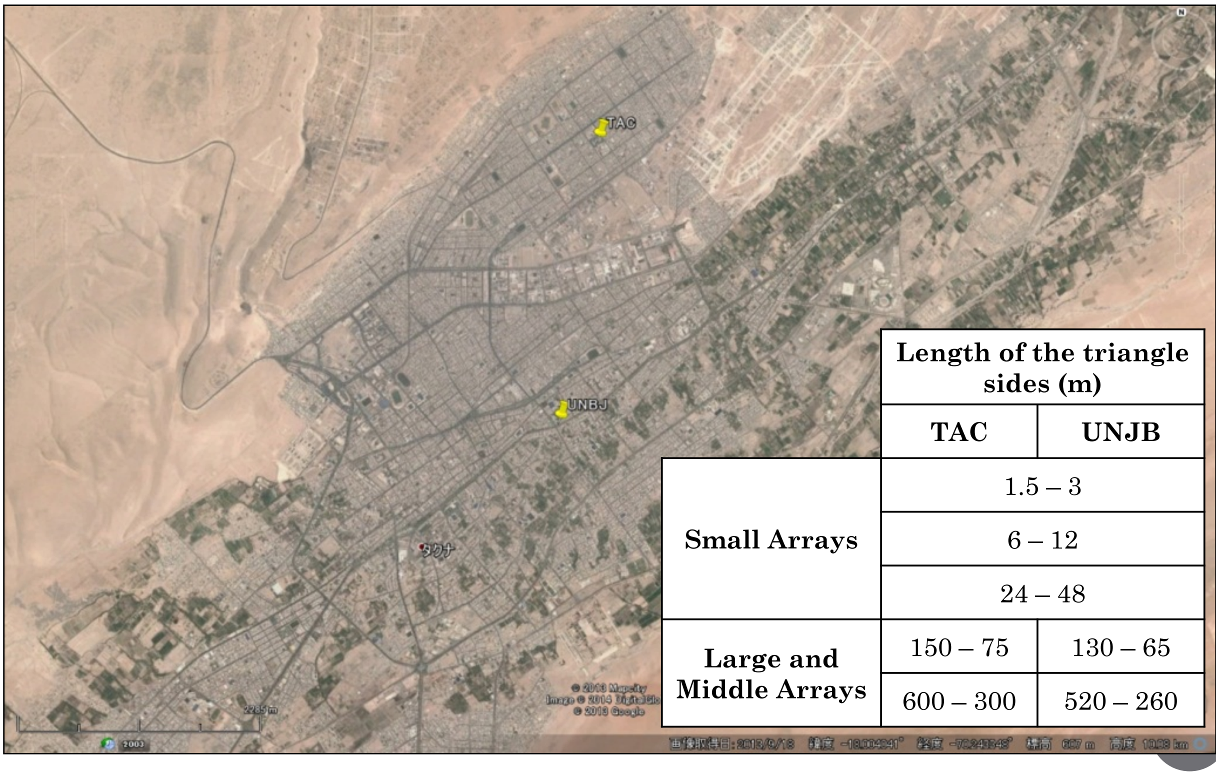

	Length of the triangle sides (m)	
	TAC	UNJB
Small Arrays	1.5 – 3	
	6 – 12	
	24 – 48	
Large and Middle Arrays	150 – 75	130 – 65
	600 – 300	520 – 260

Microtremors array measurements

Inversion using dispersion curve at TAC

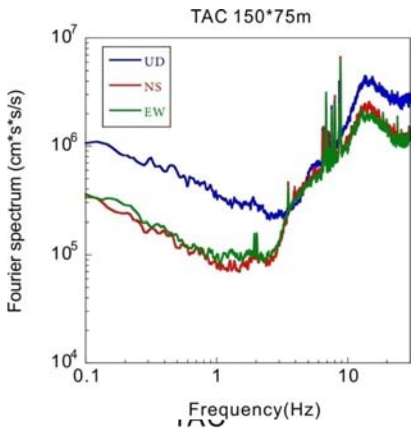

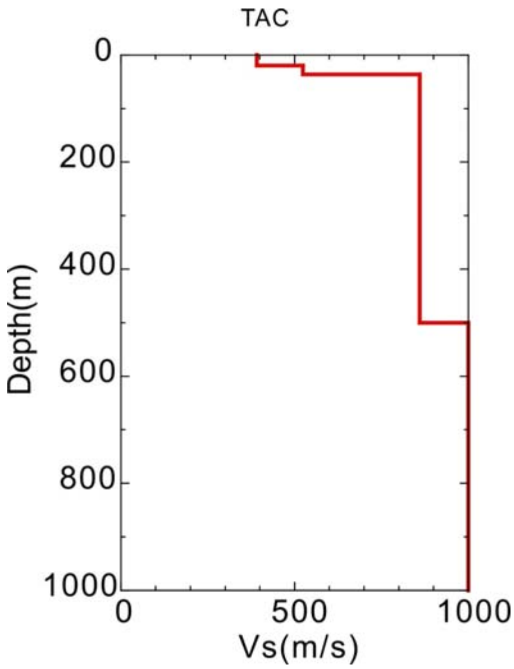

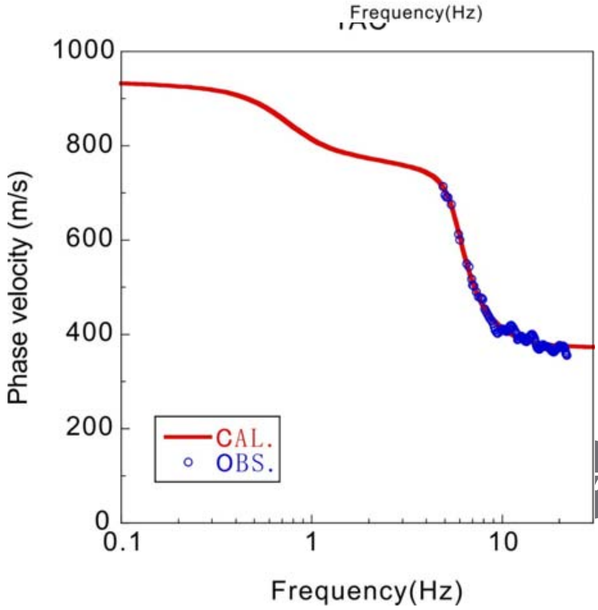

3. Receiver function from earthquake records (1/4).

- UPT (Private University of Tacna)

Jan. 29, 2014 M_L=5.4   Dep.120km

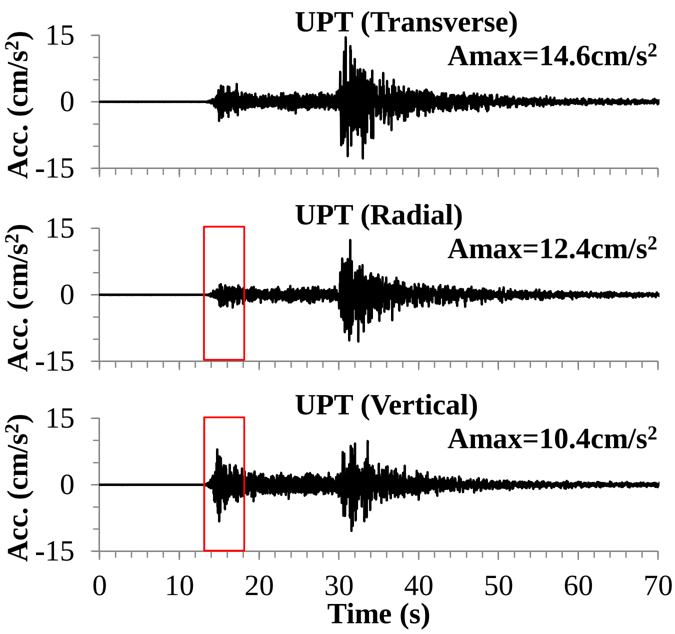

Figure 1. Acceleration seismograms observed at UPT.

In the calculation of the receiver function at UPT, we used the first 5 seconds from the onset of the P-wave (13.2s) in radial and vertical component records.

Receiver function (Langston, 1979) :

$$R(\omega) = D_{rad}(\omega) D^{*}_{ver}(\omega) G(\omega) / \Phi(\omega)$$

$$\Phi(\omega) = \max\{D_{ver}(\omega) D^{*}_{ver}(\omega), c \cdot \max[D_{ver}(\omega) D^{*}_{ver}(\omega)]\}$$

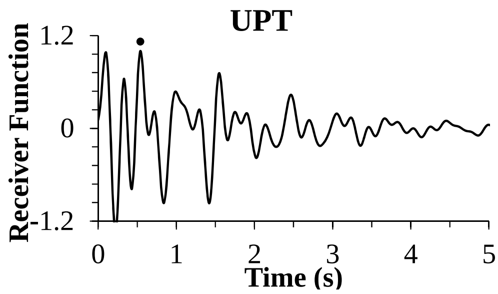

Figure 2. Observed receiver function at UPT. A solid circle attached indicates an observed PS-P time (arrival times of PS waves). A band-pass filter with a frequency range from 0.2 to 5.0Hz was applied.

3. Receiver function from earthquake records (3/4).

- TAC

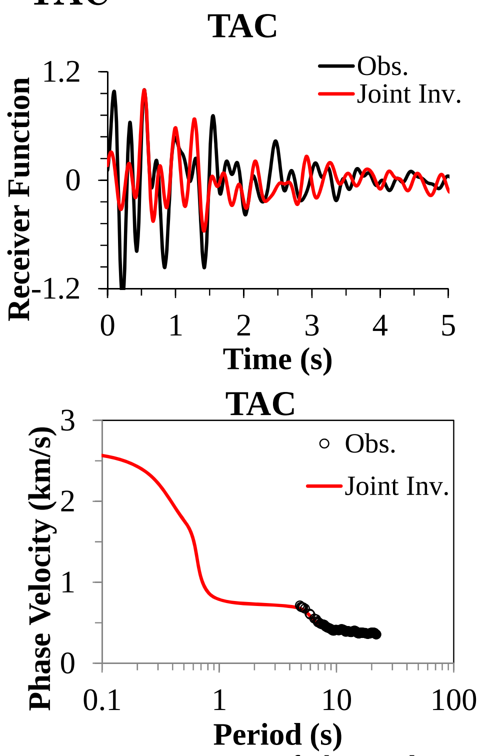

Figure 5. Comparisons of observed receiver function and Rayleigh-wave phase velocity with theoretical ones from the joint inversion.

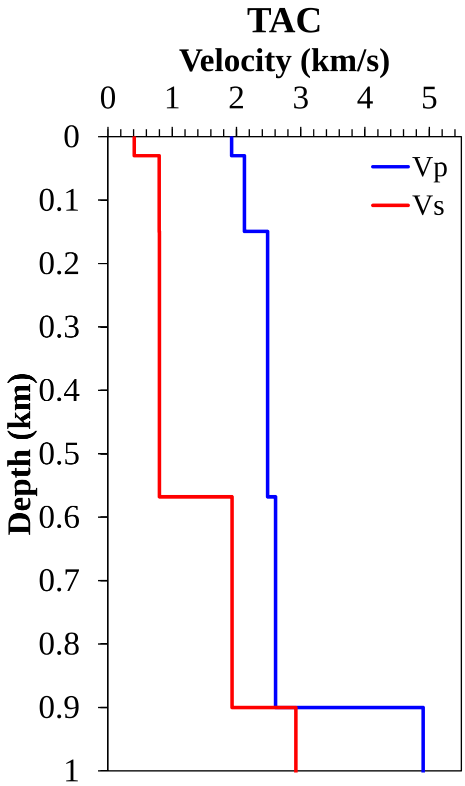

Figure 6. Inverted P and S-wave velocity profile at TAC.

Thank you for your kind attention